Fluorinated Graphdiyne Under Strain: A First-Principles Study of electronic and optical properties

N Saghir[1], G J Rampho[1] and M Khenfouch[2]

[1]Department of Physics, University of South Africa (UNISA), 28 Pioneer Ave Florida Park Roodepoort, Johannesburg, South Africa.
[2]Materials, Electrical Systems, Energy and Environment Laboratory (LMS3E), Materials and Energy Engineering group, Faculty of Applied Sciences, Department of Applied Physics, Ait Melloul, Ibn Zohr University, 86153 Agadir, Morocco.

E-mail: 58564160@mylife.unisa.ac.za

Abstract. Fluorine-doped graphdiyne, a modified two-dimensional carbon allotrope, offers promising tunability of electronic properties for flexible electronics and optoelectronic applications. Using first-principles calculations based on density functional theory, this study systematically investigates the influence of tensile strain on the electronic and optical properties of fluorine-doped graphdiyne. The results reveal that the fluorine-doped graphdiyne exhibits a direct band gap that is highly sensitive to mechanical strain. Under biaxial tensile strain, the band gap increases progressively with increasing strain, indicating effective modification. Additionally, tensile strain enhances the structural stability of the 4% and 8% biaxial strain framework. Furthermore, the optical absorption of the strained fluorine-doped graphdiyne. is enhanced under strain, particularly in the visible range, making it a promising candidate for flexible optoelectronic and photovoltaic applications.

1 Introduction

Graphdiyne (GDY), a novel two-dimensional (2D) carbon allotrope composed of sp and sp^2-hybridized carbon atoms, has garnered significant attention for its unique electronic structure, natural band gap, and high carrier mobility [1,2]. Unlike graphene, GDY possesses a direct band gap (~0.46 eV), making it inherently suitable for electronic and optoelectronic applications [3]. Due to its porous structure and chemical versatility, GDY has shown potential in a wide range of fields, including energy storage [4], catalysis [5], gas separation [6], and nanoelectronics [7].

Heteroatom doping is an effective strategy to tailor the electronic, chemical, and structural properties of GDY. In particular, fluorine doping introduces strong electron-withdrawing effects, modifies charge density distributions, and induces new electronic states near the Fermi level [8, 9]. These modifications can enhance chemical reactivity and enable precise control over GDY's semiconducting behaviour.

Additionally, strain engineering is a widely used technique to tune the band structure of 2D materials without altering their chemical composition [10, 11]. Applied tensile or compressive strain can significantly impact charge transport, band dispersion, and stability. While pristine and doped GDY have been studied under strain [12], the combined effect of fluorine doping and mechanical deformation remains unexplored.

This work investigates the electronic and optical properties of fluorine-doped GDY (C_16 F_2) (FGDY) under biaxial strain using density functional theory (DFT). By systematically analyzing strain-induced changes in the band structure, DOS and absorption, we demonstrate how doping and strain synergistically tune the optoelectronic characteristics of GDY, providing valuable insights for its use in flexible electronics, strain sensors, and adaptive optoelectronic devices.

2 Computational details

First-principles calculations were conducted using the CASTEP module within the Materials Studio framework [13], based on density functional theory (DFT). The GGA-PBE functional was employed for geometry optimization, while the HSE06 hybrid functional was used to more accurately predict electronic band structures due to GGA's known underestimation of band gaps [14]. Spin effects were neglected in all simulations. A plane-wave cutoff energy of 450 eV and a 6×6×1 Monkhorst–Pack k-point grid were used for Brillouin zone sampling. To simulate isolated monolayers, a 15 Å vacuum was added along the Z-axis, which is normal to the graphdiyne plane. The system was fully relaxed with convergence criteria of 2.0×10^{-6} eV/atom for total energy and 0.05 eV/nm for atomic forces. All electronic property analyses were based on these relaxed structures [15].
A 2×2×1 supercell was constructed and mechanical strain was introduced by varying the lattice along biaxial in-plane direction. To prevent full relaxation negating the imposed strain, atomic positions were fixed in position.

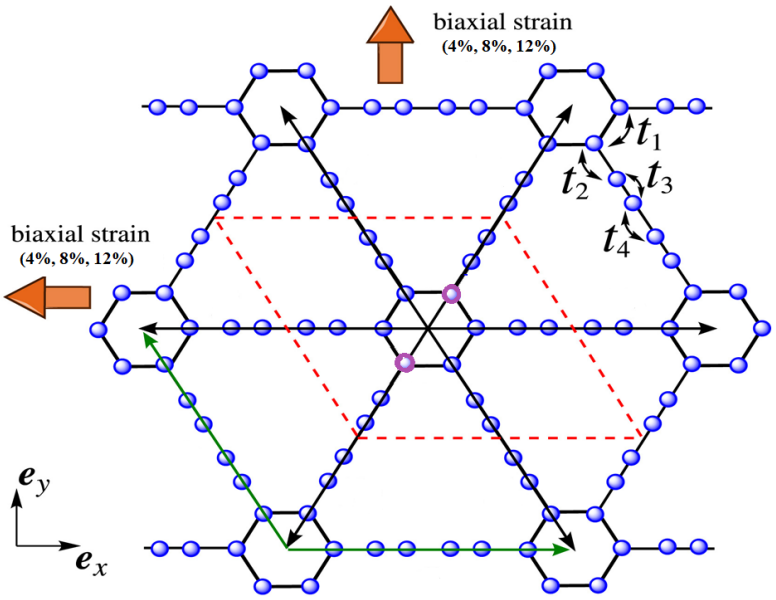

Figure 1: Atomic structure of graphdiyne, with arrows indicating the directions of applied symmetrical biaxial tensile strain.

3 Results and discussions

3.1 Geometrical Structures

To determine the structures stability, we calculated the formation energies of the strained structure. The computed results are displayed in Table 1.

Strain type	Lattice constant (Å)	Band gap (eV)	Formation energy (eV)
Unstrained	18.762	0.75	-2.93
Biaxial 4%	19.512	0.82	-3.05

Biaxial 8%	20.263	1.13	-3.13
Biaxial 12%	21.013	1.98	-2.72

Table 1: The calculated formation energies of the strained FGDY structure.

As seen in Table 1, 8% biaxial strained structure has the highest formation energy followed by 4% biaxial strained structure which has the formation energy -3.05 eV. The formation energy of the 12% strain structure indicates the lowest stability. The negative values of the formation energy demonstrates that the structures are energetically stable.

3.2 Electronic Properties

The combined effect of fluorine doping, along with applied strain, alters the lattice parameters and atomic configuration of graphdiyne, thereby significantly influencing its electronic properties.

3.2.1 Band Structures and Density of states Figure 2 illustrates the electronic band structures of pristine and biaxial strained graphdiyne (FGDY) under 4%, 8%, and 12% strain, and computed using the hybrid HSE06 functional, which is known for yielding more accurate band gap predictions [15]. A dense k-point grid of 40×40×1 was employed to ensure convergence of the electronic properties. As shown in Fig. 2(a), the unstrained GDY exhibits a direct band gap of 0.760 eV. Upon applying 4% biaxial strain, Fig. 2(b) reveals a slight increase in the band gap to 0.831 eV, maintaining its direct nature. At 8% strain, as illustrated in Fig. 2(c), both the conduction band minimum (CBM) and valence band maximum (VBM) remain located at the K-point, confirming a direct band gap of 1.120 eV. Further increasing the strain to 12% significantly widens the band gap to 1.981 eV, as seen in Fig. 2(d). Among all configurations, 12% strained FGDY shows the largest band gap, followed by 8% and 4%, with the unstrained structure having the smallest band gap.

Figure 2 also presents the total density of states (DOS) for graphdiyne (GDY) subjected to varying levels of biaxial tensile strain: 0% (unstrained), 4%, 8%, and 12%. In the unstrained state (Fig. 2(a)), FGDY exhibits a clear semiconducting nature, as evidenced by the absence of electronic states at the Fermi level. The calculated band gap is 0.760 eV, consistent with the direct band gap observed in the corresponding band structure. Upon applying 4% biaxial strain (Fig. 2(b)), the band gap increases slightly to 0.831 eV, and the Fermi level remains within the energy gap, indicating that the material maintains its semiconducting character. This strain induces a subtle shift in the electronic structure, but no mid-gap states are introduced. As strain increases to 8% (Fig. 3(c)), the DOS shows a further widening of the gap, exhibiting an energy gap of 1.120 eV. An absence of states near the Fermi level confirms that the system remains a direct band-gap semiconductor. Finally, under 12% biaxial strain (Fig. 3(d)), FGDY demonstrates a significantly larger band gap of 1.981 eV. The DOS profile shows a well-defined gap with no states at the Fermi level, indicating a robust semiconducting behaviour even under high strain. These results, in agreement with the band structure plots, demonstrate that biaxial tensile strain systematically increases the band gap of FGDY without inducing metallicity. The gradual increase in the band gap with strain is attributed to the stretching of C–C bonds and changes in orbital overlap, which reduce the interaction between the valence and conduction bands. This tunability in the electronic structure highlights the potential of strained FGDY for strain-engineered electronic and optoelectronic applications.

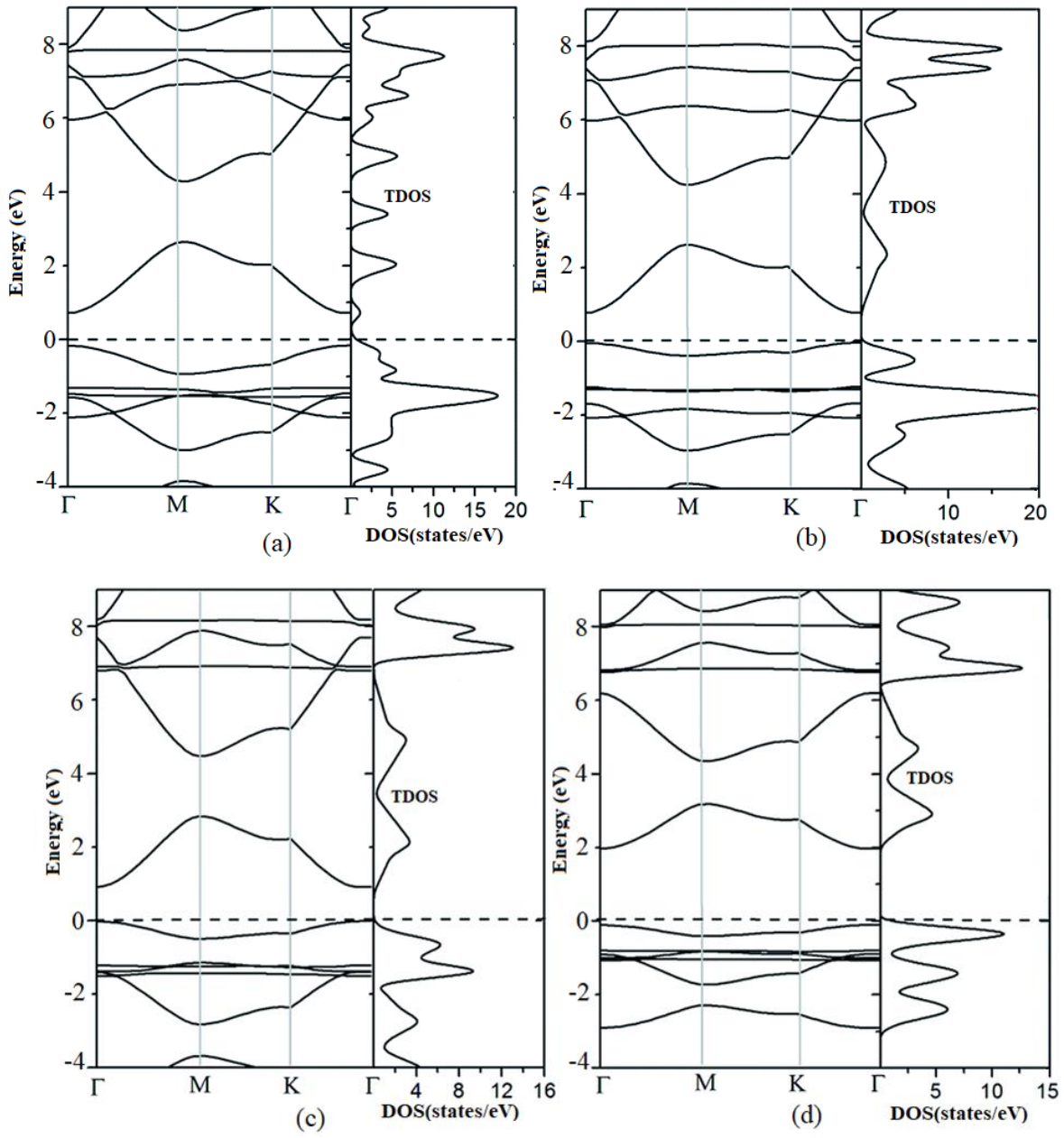

Figure 1: Total density of states and band gap images of (a) Unstrained GDY (b) 4% Biaxial-strained GDY (c) 8% Biaxial-strained GDY and (d) 12% Biaxial-strained GDY.

3.3 Optical Properties

3.3.1 Absorbance and Dielectric function Now, we analyse the optical response of fluorine-doped graphdiyne. A real as well as imaginary component of the dielectric function for both the unstrained and strained (with a strain of 4%, 8% and 12%) C12F2 monolayers were computed for light polarized in-plane along the x- and y-directions. These results are presented in Figure 4. It is evident that the optical spectra of the 8% and 12% biaxially strained monolayers exhibit isotropy with respect to light polarized along the x- and y-axes, whereas unstrained and 4% biaxial strain induces anisotropy. Furthermore, for all structures, the optical response demonstrates significant anisotropy within the in-plane directions. For the biaxial 8% monolayer, the first peak in the imaginary part of the dielectric function, Imε_αβ (ω), occurs at 1.15 eV for light polarized within the plane. Noticeably, applying biaxial strain 4%, 8% and 12% causes a slight blue shift (shift to higher energy) of the absorption edge

in Imε for E∥x at low frequencies. Conversely, the absorption edge of Imε for E∥y shifts toward lower energies under 4% biaxial strain. Along the E∥x direction, the $C_{16}F_2$ monolayer exhibits a static dielectric constant (Reε_0) of 3.71. Under 12% biaxial strain, Reε_0 decreases in all polarization directions. Under 12% biaxial strain, the static dielectric constant rises in the E∥x direction but drops in the E∥y direction. Figure 5 displays an absorption coefficient, α_{ij} (ω), for each polarization direction. Under in plane polarization, both the unstrained and strained C16F2 monolayers exhibit their first absorption band between 1.08 eV and 1.48 eV, falling in the infrared to near infrared region. This initial peak originates at the Γ point and arises from electron transitions between 1C dominated valence states and F dominated conduction states. A second absorption band appears near 1.78 eV for both x and y directions for every structure examined, placing it within the visible range—an energy window well suited to optoelectronic applications. The most intense absorption feature for in plane polarization is broad, extending over approximately 3.41 eV to 5.19 eV.

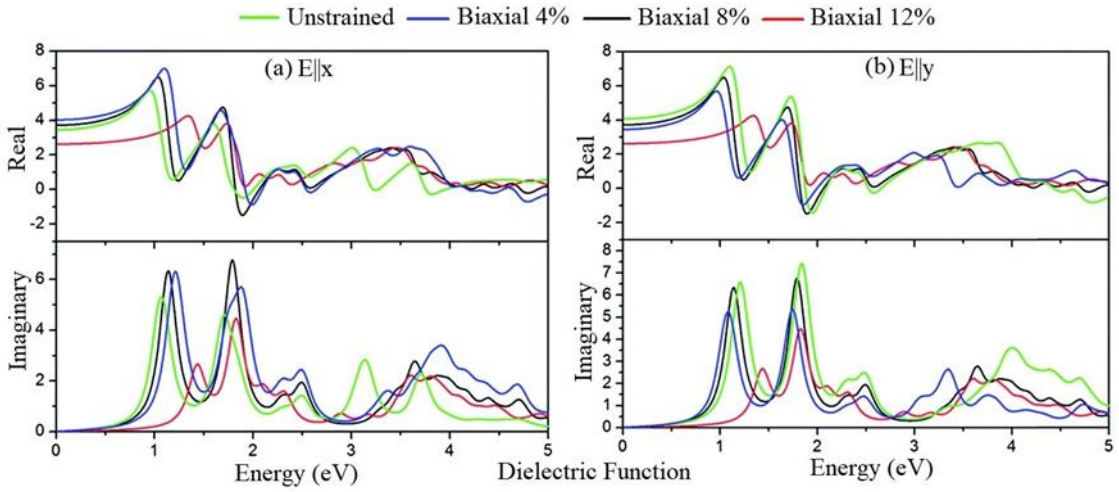

Figure 1: Graphs of Dielectric function for monolayer FGDY unstrained and with biaxial strain (4%, 8%, and 12%) For light polarized within the plane along the x and y directions.

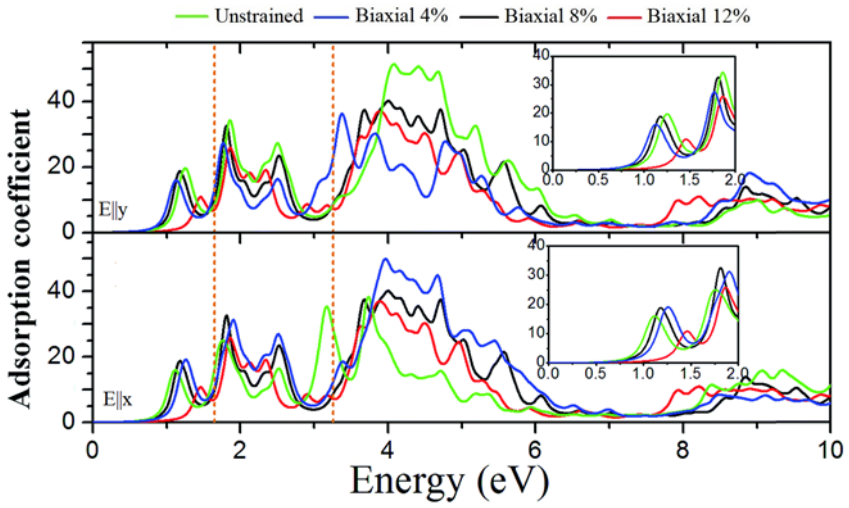

Figure 1: Graph of Absorption coefficient for monolayer FGDY unstrained and with biaxial strain (4%, 8%, and 12%) for the in-plane (E||x and E||y) light polarizations.

4 Conclusion

The present study investigates how fluorine doping under biaxial strain influences the electronic and optical behavior of graphdiyne (FGDY) using first-principles DFT calculations. The results demonstrate that FGDY possesses a tunable direct band gap, which increases systematically with the application of strain—from 0.76 eV

(unstrained) to 1.98 eV at 12% biaxial strain—highlighting its strong strain-dependent electronic characteristics. This band gap modulation is attributed to the strain-induced elongation of C–C bonds and modified orbital interactions that reduce overlap between the valence and conduction bands.

The structural stability of FGDY improves under moderate strain, as evidenced by the increasingly negative formation energies at 4% and 8% strain. However, beyond 8%, a decrease in formation energy suggests a threshold beyond which stability begins to diminish. Optical analysis further reveals that strain not only enhances light absorption but also causes notable shifts in the dielectric function and absorption spectra. In particular, biaxial strain induces a blue shift in the absorption edge for E∥x polarization, while the dielectric response becomes increasingly isotropic at higher strain levels. The strong and broad absorption in the visible range (1.80–5.19 eV) under strain underscores the potential of FGDY for optoelectronic applications.

Overall, the synergistic effects of fluorine doping and mechanical strain offer an effective approach for engineering the band structure and optical response of graphdiyne, making FGDY a promising candidate for flexible electronics, strain sensors, and next-generation optoelectronic devices.

References

[1] D. Malko, C. Neiss, F. Viñes, and A. Görling, "Competition for graphene: Graphynes with direction-dependent Dirac cones," *Phys. Rev. Lett.*, vol. 108, p. 086804, 2012.

[2] G. Li, Y. Li, H. Liu, Y. Guo, Y. Li, and D. Zhu, "Architecture of graphdiyne nanoscale films," *Chem. Commun.*, vol. 46, pp. 3256–3258, 2010.

[3] M. Long, L. Tang, D. Wang, Y. Li, and Z. Shuai, "Electronic structure and carrier mobility in graphdiyne sheet and nanoribbons: Theoretical predictions," *ACS Nano*, vol. 5, no. 4, pp. 2593–2600, 2011.

[4] S. Zhang, M. Xie, F. Li, Z. Yan, H. Zhang, J. Wang, and Y. Liu, "Semiconducting group 15 monolayers: A broad range of band gaps and high carrier mobilities," *ACS Appl. Mater. Interfaces*, vol. 8, no. 13, pp. 8467–8473, 2016.

[5] X. Gao, H. Liu, D. Wang, and Y. Li, "Graphdiyne: A promising carbon allotrope for versatile applications," *Nat. Commun.*, vol. 3, p. 884, 2012.

[6] Y. Yang, Y. Guo, and Y. Zhao, "Modulating the band gap and carrier mobility of graphdiyne through chemical doping," *J. Phys. Chem. C*, vol. 123, no. 18, pp. 11048–11054, 2019.

[7] Y. Xu et al., "Ultrathin graphdiyne membranes for efficient hydrogen separation," *Nat. Nanotechnol.*, vol. 13, pp. 766–772, 2018.

[8] H. Wang, Q. Li, and L. Yang, "Strain engineering of electronic and optical properties in graphdiyne," *Physica E*, vol. 121, p. 114064, 2020.

[9] Z. Cui, X. Tian, Z. Li, Y. Hu, and S. Yang, "Tuning electronic properties of graphdiyne under strain: A first-principles study," *Carbon*, vol. 172, pp. 114–121, 2021.

[10] V. M. Pereira and A. H. Castro Neto, "Strain engineering of graphene's electronic structure," *Phys. Rev. Lett.*, vol. 103, p. 046801, 2009.

[11] Y. Wang, C. Cong, and T. Yu, "Raman spectroscopy study of mechanically strained monolayer graphene," *Nano Res.*, vol. 7, pp. 441–449, 2014.

[12] J. Liu, Y. Wang, W. Li, Z. Wang, and J. Wang, "Strain-dependent electronic and optical properties of monolayer black phosphorus," *J. Appl. Phys.*, vol. 121, p. 185701, 2017.

[13] B. Tang, Q. Luo, Q. Zhang, Z. Wu, and Z. L. Ran, "First-principles study of strained graphyne structures," *J. Synth. Cryst.*, vol. 43, pp. 1269–1274, 2014.

[14] J. P. Perdew, K. Burke, and M. Ernzerhof, "Generalized gradient approximation made simple," *Phys. Rev. Lett.*, vol. 77, pp. 3865–3868, 1996.

[15] G. L. Liu, S. Zhou, and D. Z. Fan, "Electronic structure of strained graphdiyne," *J. Shenyang Univ. Technol.*, vol. 39, pp. 622–626, 2017.